Investigating Bleed Techniques for Aero-Optics using Water Table Flow Visualization and Numerical Simulations

William J. Koehrsen
Case Western Reserve University
Cleveland, Ohio 44106

Chung-Jen Tam
Air Force Research Laboratory/Directed Energy Directorate
Kirtland Air Force Base, NM 87113

ABSTRACT

Numerical simulations were performed to study the effects of bleed flow control for aero-optics in a Mach 2 flow around a hemispherical turret. The studies demonstrated that the bleed flow control technique can significantly decrease the unsteadiness of the flow field around the turret. The root-mean-square of optical path differences for the 45º upstream view and the 135º downstream view are reduced dramatically, improving the quality of the laser beam on the target. A bleed design methodology was also developed to reduce the overall drag of the flow path. The numerical solutions show that the bleed system with the ramp configuration works better than the other two conceptual designs. These numerical findings will be validated using a water-table flow visualization, with the experimental apparatus currently under construction at the AFRL/Directed Energy Directorate in Kirtland AFB, NM

INTRODUCTION

The propagation of laser beams through turbulent flows has been an important topic for many years, with applications ranging from missile defense to target designation and tracking. An important aspect of these applications is determining the effective beam-on-target characteristics after the beam has propagated through both the near-field turbulent flow field of the vehicle and the far-field turbulent atmosphere. Near-field propagation, or aero-optics, maintains some similarities to far-field (atmospheric) propagation, but due to the interactions between turbulence length scales, beam wavelengths, apertures, and disparity in interaction distances, the two often require different approaches to address the problems.[1,4] It is well known for aero-optics that the distortion of an optical wavefront is most severe when passing through a turbulent flow characterized by large-scale structures with strong density gradients. In addition, as the distortion is directly proportional to the density gradients, the magnitude of the problem increases with increasing Mach numbers. These types of flows are inherently three-dimensional and unsteady with high Reynolds numbers and also often exhibit flow separation.

Supersonic flow around a wall-mounted hemispherical turret, such as used in laser weapons systems, results in two distinct separated flow regions, one upstream and the other in the wake region downstream of the turret, as illustrated in Figure 1. The separated region upstream of the hemisphere near the junction of the hemisphere and the wall forms a horseshoe/necklace vortex, which wraps around the bottom of the hemisphere and moves downstream in the wake region.[5] A separate shear layer forms on the top of the hemisphere and moves downstream in the wake

region. In addition, expansion waves originate on the top of the hemisphere and are typically non-stationary. These unsteady and complex flow features pose challenges with regards to allowing laser beams to propagate through these turbulence structures without any optical aberrations.

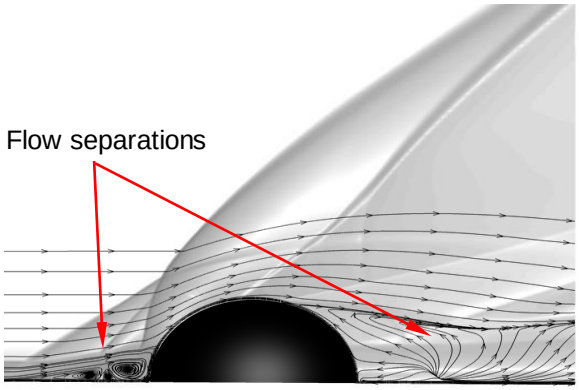

Figure 1 Schematic of the flow over a turret a supersonic speed

The objective of this study is to design a flow control system to mitigate the optical disturbances due to the strong density gradients around the hemispherical turret in a Mach 2 flow. It has previously been demonstrated that creating a cavity or "canoe" geometry for the turret to sit in can reduce the front separation bubble and position it almost entirely below the base of the turret. Moving the front bubble below the base of the turret creates an unobstructed view forward for the laser to propagate through.[6]

The current investigation into bleed control is concerned with the separation region located downstream of the turret. By sucking away the bottom of the boundary layer, a more uniform normal velocity distribution can be created, and the kinetic energy added to the fluid flow near the surface of the boundary layer can prevent flow separation. Bleed control has been successfully demonstrated in numerous applications, including the SR-71 Blackbird,[7] and scramjet applications.[8,9] Numerical studies have also shown bleeding of the flow to be an effective method of flow control for previous versions of the hemispherical turret.[6] Current work focuses on determining the optimum bleed/flow path configuration for a hemispherical turret such that a laser emanating from the turret will not suffer a severe reduction in beam quality and that will result in the smallest total pressure loss in the bleed flow path system.

EXPERIMENTAL SETUP

Experimental models of the hemispherical turrets designed with different cavity geometries can be quickly and accurately manufactured due to the capabilities of fused deposition modeling (FDM) and stereolithography (SLA), two techniques under the umbrella of 3D printing. However, the conventional wind tunnel facilities in which these models can be tested in supersonic conditions are limited and cost-prohibitive. Although numerical studies provide a preliminary representation of the flow field, it is necessary to validate the CFD results through experiments. Therefore, it is clear there exists a need for an experimental device that can bridge the gap between computational fluid dynamics (CFD) and wind tunnel testing by quickly providing a qualitative evaluation of prototype models. This device needs to be capable of validating the initial CFD studies and showing potential areas for refinement even without necessarily yielding rigorous quantitative data. The experimental device under consideration is known as a water table, and it operates by utilizing the hydraulic analogy.[10] This allows for the simulation of a 2D compressible gas flow using a relatively slow-moving free surface liquid flow, in most cases, water. Shock waves in a compressible gas flow become hydraulic jumps in the liquid flow as shown in Figure 2.

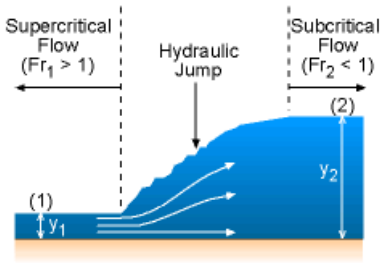

Figure 2 Hydraulic jump in free surface liquid flow

Flow enters on the left in a supercritical, or equivalently, supersonic state, with a Froude number greater than 1. The flow then encounters an obstacle, and much as a compressible flow is compressed and forms a shock wave, the water is forced to undergo a jump, or a gain in height relative to the incoming flow. The resulting downstream flow is now subcritical with a Froude number less than 1, or equivalently, subsonic with a Mach number less than 1. While a shock wave converts kinetic energy into thermal energy, a hydraulic jump converts the kinetic energy of the incoming flow into gravitational potential energy, hence the height increase of the flow.

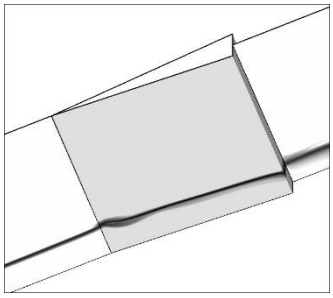

Figure 3 Shadowgraph showing hydraulic jump around a wedge in a numerical simulation

The Froude number, the free surface liquid flow analogy to the Mach number, is the velocity of the flow divided by the ideal wave velocity of a surface wave, where h in (1) is the height above the reference surface and g is the acceleration due to gravity.[11]

$$Ideal\ wave\ velocity = \sqrt{gh} \tag{1}$$

$$Froude\ Number = \frac{u}{\sqrt{gh}} \tag{2}$$

$$Mach\ Number = \frac{u}{\sqrt{\gamma RT}} \tag{3}$$

Furthermore, using the continuity equation, the momentum equation, and the energy equation, it is possible to derive relationships between the height of the liquid before and after the hydraulic jump and the density, temperature, and pressure ratios before and after a shock wave.[11]

$$\frac{\rho}{\rho_o} = \frac{h}{h_o} \tag{4}$$

$$\frac{T}{T_o} = \frac{h}{h_o} \tag{5}$$

$$\frac{p}{p_o} = \left(\frac{h}{h_o}\right)^2 \tag{6}$$

These relations allow for quantitative data to be obtained using a water table, although with significant limitations. From the isentropic flow relations (7), it can be demonstrated that the hydraulic analogy is only valid for a compressible gas with an adiabatic index of 2.0.[12]

$$\frac{p}{p_o} = \left(\frac{T}{T_o}\right)^{\frac{\gamma}{\gamma-1}} = \left(\frac{h}{h_o}\right)^2 \tag{7}$$

As air can be treated as an ideal gas with a constant adiabatic index of 1.4 under the conditions being investigated, the hydraulic analogy is not intended to be used for rigorous data collection. **Figure 4** demonstrates the effect of changing the adiabatic index (defined as the ratio of specific heat at constant pressure to the specific heat at constant volume) on the pressure ratio as a function of Mach number.

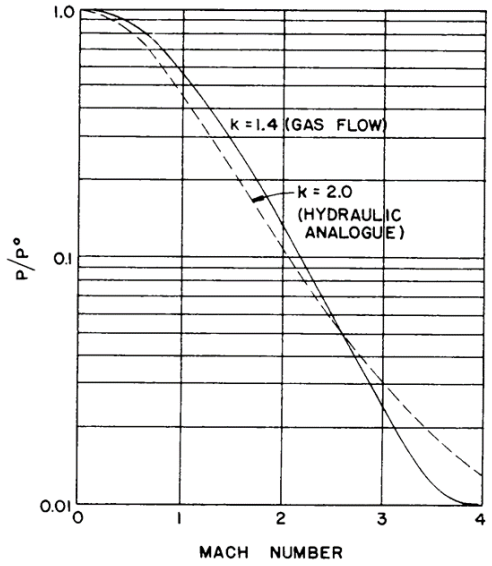

Figure 4: Pressure ratio versus Mach number with varying specific heat ratio[13]

The proposed water table has been developed as a qualitative tool only. Quantitative measurements for the most promising hemispherical turret cavity geometries can be obtained from the conventional method of wind tunnel tests. Although the flow field around a hemispherical laser turret is inherently three-dimensional, the two-dimensional water table visualization will be able to capture enough flow features to validate the numerical studies that have been performed on the prototype. The commonly used technique of oil flow visualization in wind tunnels is also two-dimensional, but from previous characterizations of the flow field, it is possible to extract valuable information from this technique. Prior knowledge of the flow field along with CFD will allow the water table to provide validation despite not yielding rigorous numbers. Neither the water table nor CFD is entirely to be relied upon in isolation, but by using these two tools concurrently, it is possible to assess the suitability of prototypes.

A conceptual drawing of the proposed water table at the Air Force Research Laboratory/Directed Energy Directorate (AFRL/RD) is shown in Figure 5. All of the main components are represented except for the pump and associated piping. The main concern of the water table design was the test section. It was decided that polycarbonate, known by the trade name Lexan, would be the ideal material for the surface of the test section, as it is lighter than glass, and has a refractive index of 1.58 which is comparable to that of crown glass at an index of refraction of 1.52.[14] The test section itself is 3 feet wide by 5 feet long. One potential issue was the interference of the boundary layer that grows along the side walls with the flow field visualization around the model, particularly the shock waves or hydraulic jumps originating at the leading edge of the model. Therefore, numerical studies on a simple wedge were conducted at Mach numbers of 1.5 and 2.0 with a water height of 0.4 inches to assess the correct dimensions for the test section. These figures represented the maximum flow condition for which the water table was expected to function. Density shadowgraphs of the resulting flow field can be seen in Figure 6. Based on the numerical studies, the 3 feet wide by 5 feet long dimensions of the water table were deemed appropriate for the intended studies as the boundary layer did not interfere

with the flow field until some distance downstream of the model. As the flow is supercritical, the interference occurring downstream of the model will not be able to propagate upstream and thus will not affect the flow field visualization of the shocks around the turret model.

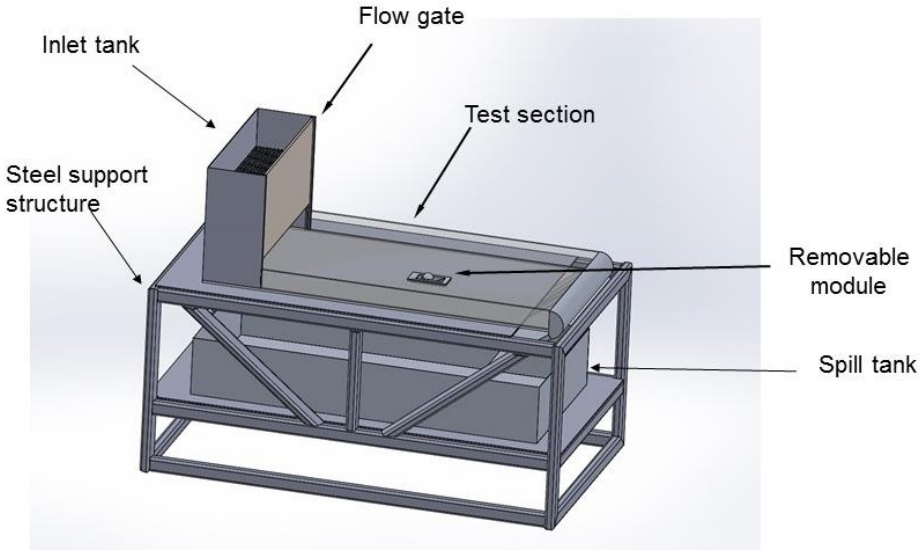

Figure 5 Conceptual design of water table apparatus at AFRL/RDL

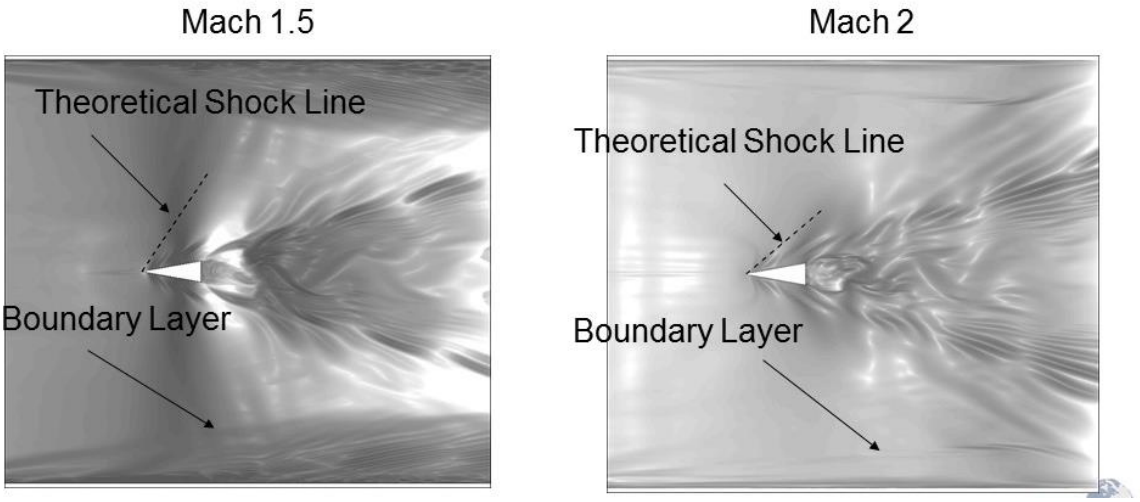

Figure 6 Density shadowgraphs demonstrating shock waves and boundary layer growth

The maximum flow rate occurs with 0.4 inches of water at a Froude number or Mach equivalent of 2.0.

$$Fr = 2.0 = \frac{u}{\sqrt{32.2\frac{ft}{s} * \frac{0.4\ in}{12\frac{in}{ft}}}},\ u = 2.147\ ft/s \tag{8}$$

$$\dot{m} = \rho A u = 62.4\frac{lb}{ft^3} * \left(\frac{0.4in}{12\frac{in}{ft}} * \frac{36\ in}{12\frac{in}{ft}}\right) * 2.147\frac{ft}{s} = 13.4\frac{lb}{s} \tag{9}$$

$$Gallons\ per\ minute = \frac{13.4\frac{lb}{s}}{8.35\ lb/gal} * 60\frac{s}{min} = 94.5\ gpm \tag{10}$$

As can be seen in Eqs. (8)-(10), the maximum flow rate on the table corresponds to a requirement for a water pump with a capability of pumping 95 gallons per minute assuming no losses. A centrifugal pump is optimal for the water table because it can provide a smooth flow and will not introduce disturbances into the flow that would affect the characterization of the streamlines around the turret. In addition, mesh screens can be placed in the inlet tank to ensure that the flow entering the test section is free of disturbances. The pump should be isolated from the water table and placed on a separate stand with vibration-absorbing pads. The lack of mechanical complexity in the overall design of the water table results in a comparatively cost-effective experimental apparatus that still allows for accurate qualitative representations of compressible flow.

Removable Hemispherical Turret Model

As the objective of the water table is to facilitate the rapid evaluation of prototype hemispherical turret models, the water table was designed to allow for a removable model that could be easily switched. To that end, the polycarbonate testing surface was designed with a flange that would allow the model to be placed in the liquid, with the base of the rounded turret flush with the surface of the liquid. Placing the model in the water table from above eliminated the need for a complex support system below the table, and should allow for rapid switching of models. The models themselves are designed to allow for the insertion of dye into the flow to visualize streamlines. Moreover, the rear of the model in Figure 7 shows one potential configuration for bleed control. The models themselves have several features, including sharp corners and small dye ports that do not allow for conventional manufacturing options such as milling or turning on a lathe. However, additive manufacturing techniques, under the umbrella term 3D printing, have proven to be well-suited to quickly building these prototypes. Two different methods of 3D printing can be utilized to make the models. Fused deposition modeling (FDM), creates pieces by extruding a material, most often plastic, one layer at a time onto a surface with the piece built layer by layer from the bottom up. For this application, FDM is the quicker method, but it leaves a rougher surface finish and cannot adequately form the required small dye holes which must be drilled out after printing. A second option is known as stereolithography (SLA). SLA works through the process of photopolymerization in which a light of a specific wavelength emanates into a resin bath and selectively causes molecules to join together into chains, or polymerize, creating a rigid shape. SLA can rapidly produce parts, but after emerging from the resin bath, the manufactured pieces need to be cured in ultraviolet light for up to a week to ensure structural rigidity. The main advantage of SLA printing is that it allows for more detailed shapes and can create a smoother surface finish. Additive manufacturing greatly reduces the time-scale for the creation of a model, and new prototypes can move from a theoretical idea to a 3D CAD model to a physical model within several days.

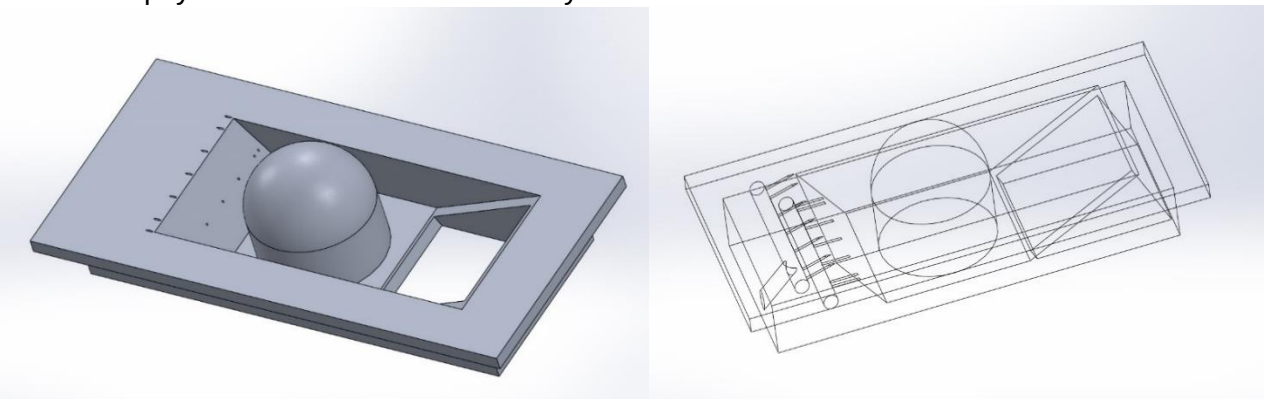

Figure 7 CAD model of fourth generation hemispherical turret with bleed

NUMERICAL APPROACH

Three-dimensional, steady-state, numerical simulations using Loci-Chem[15,16] were performed to understand the effectiveness of the conceptual bleed devices for aero-optics research. Loci-Chem is a density-based, finite volume code which is capable of handling mixed element type unstructured grids. The convective fluxes are based on Roe's flux difference splitting. Both convective and diffusive fluxes are evaluated to second order accuracy. The Menter-SST two-equation turbulence model was used for the steady simulations, and the hybrid RANS/LES turbulence model was employed for the unsteady simulations.

DESIGN METHODOLOGY FOR THE BLEED DEVICE

As mentioned earlier, the objective is to design a flow control system to mitigate the optical disturbances due to strong density gradients around the hemispherical turret at a Mach 2 flow. The first conceptual bleed or slot design for a 2" hemispherical turret was based on the incoming boundary layer thickness, 0.25". Therefore the width of the opening is 2.5″ or 1.25 D, where D (= 2″) is the diameter of the turret, as shown Figure 8. The depth of the device is set to be 1" (0.5 D). The number of openings in the streamwise direction behind the turret was based on trial-and-error approach. The best performance, in terms of reduction of the separation or wake region, was having the slots 8, 9, 11, 13, and15 opened to let the air pass through into the bleed region below (Figure 8).[6] This result will be discussed in the next section.

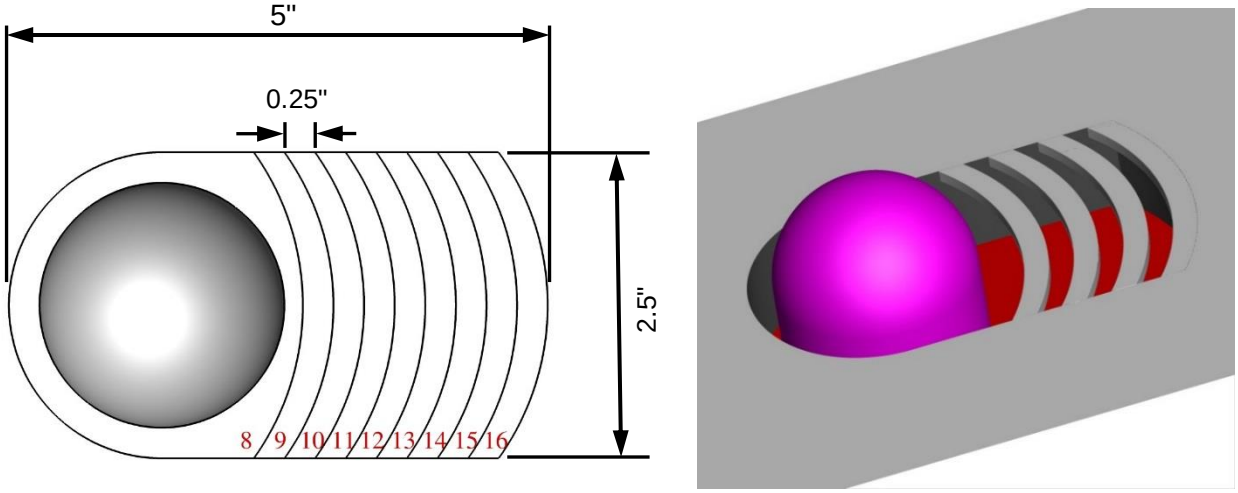

Figure 8 Dimensions and 3-D view of the first conceptual bleed/slot design

A physics-based methodology was developed to optimize the bleed internal flow path to reduce the drag of the system, instead of based on trial-and-error manner. The width, depth, and length of the bleed system were determined based on the flow physics of the supersonic flow over the hemispherical turret, as illustrated in Figure 9. The origin of the x-, y- and z-axes is located on the base of the center of the turret. Similar to the first bleed design, the width (a = 0.625 D) is based on the incoming boundary layer thickness. The depth (b) is determined using the area-Mach relationship between Mach 1.7 and 2, which gives b equal to 0.5 D. Note that Mach 1.7 is the mass-averaged Mach number behind the turret. The distance, x_1 (= D), is computed using the Mach 2 expansion wave relationship, and x_2 = 1.635 D is determined based on the oblique shock relationship between Mach 1.7 and 2. Therefore the total length of the bleed system is equal to 2.635 D. Although this analogy is based on an inviscid flow assumption, the bleed flow path design is scalable based on the turret diameter, incoming boundary layer thickness and Mach number.

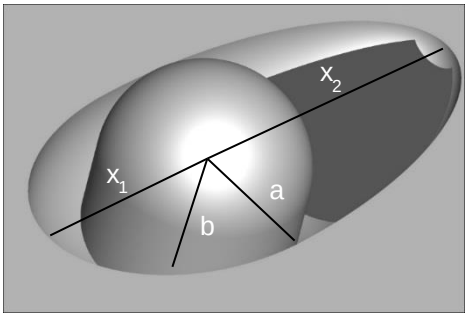

Figure 9 Dimensions of the bleed flow path design

RESULTS AND DISCUSSIONS

The water-table apparatus is still under construction at AFRL/Directed Energy Directorate, therefore no flow visualization will be presented in this report. However, the performance of the conceptual bleed device for aero-optics will be discussed based on the numerical simulations. Figure 10 shows the instantaneous density contours with and without the bleed system. This bleed configuration was the first conceptual design studied (Figure 8). Without the bleed, the unsteady density fluctuations can be distinctly observed in front of the turret and in the wake region behind the turret (Figure 10a). In addition, the separation region/horseshoe vortex is visible around the turret. These unsteady flow features are dramatically decreased with the bleed device, as depicted in Figure 10b. Thus, the degradation of the laser beam is significantly reduced with this flow control system.

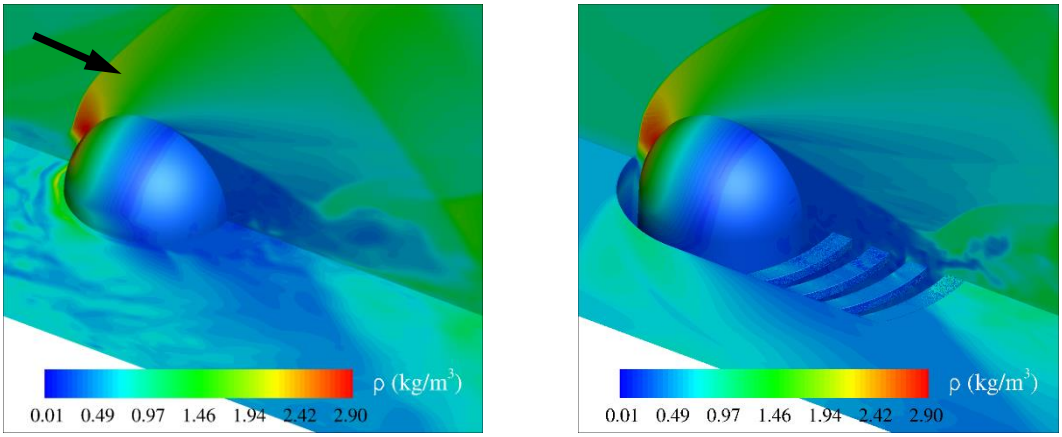

a) without bleed b) with bleed

Figure 10 Instantaneous density contour images

Figure 11 shows the numerical shadowgraph images at a height of 0.4” away from the bottom wall to mimic the water-table flow visualization. There are two distinct density gradients in front of the turret without the bleed control (

Figure 11a). The density gradient farther upstream of the turret is the shock structure due to the separation region, and the density gradient closer to the turret is the bow shock caused by the hemispherical turret. Similar flow features were observed from the previous experimental and numerical studies.[5] In addition, the wake region is visible behind the turret. With the bleed system, the separation region in front of the turret has diminished thus the shock system has reduced to one bow shock, as illustrated in

Figure 11b. The wake region behind the turret has also decreased with the addition of the bleed technique. Due to the discrete bleed slot configuration (Figure 8), additional density gradients/waves can be seen behind the turret. Despite this flow disturbance, the bleed system not only reduces the size of the wake region but also decreases the unsteadiness of the flow structures around the turret. Once the water-table flow visualization is available, the numerical studies can be validated and compared with the realistic physical phenomenon.

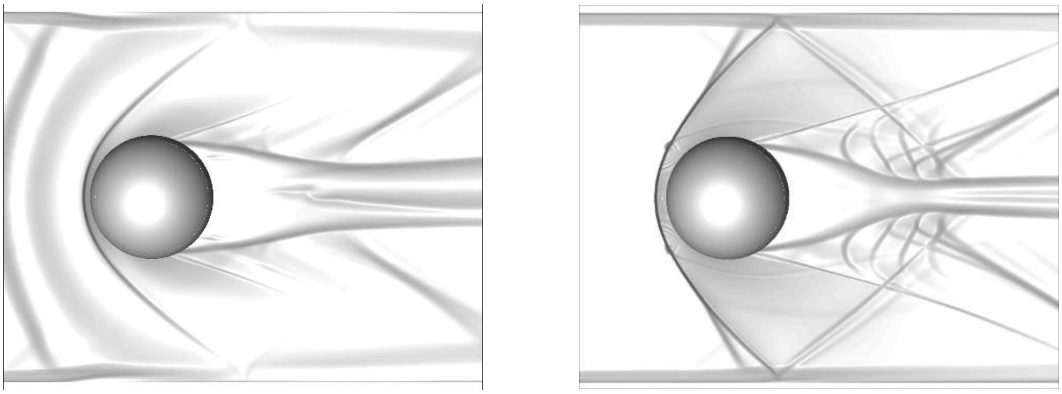

a) without bleed b) with bleed

Figure 11 Top view of the numerical shadowgraph images

Quantitative evaluations of the bleed system for the aero-optics were compared in terms of the root-mean-square of the optical path difference (OPD) at two different viewing angles. Figure 12 shows the OPD_{rms} looking 45° upstream of the hemispherical turret. With the bleed system, the OPD_{rms} map is not only more uniform, but also the minimum value has decreased by two orders of magnitude compared to the OPD without flow control. Thus, these results indicate that the degradation of the laser beam is dramatically reduced by the bleed control method.

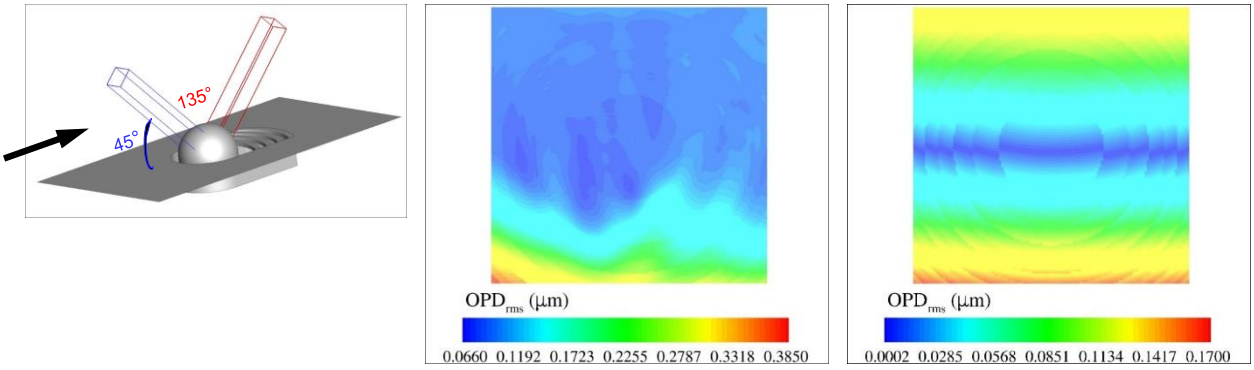

a) without bleed b) with bleed

Figure 12 Root-mean-squared of OPD at 45° viewing angle

Figure 13 illustrated the OPD_{rms} looking 135° downstream of the hemispherical turret. Although the OPD_{rms} map with the bleed system (Figure 13b) is not as uniform compared to the flow patterns looking 45° forward (Figure 12b), the minimum value of OPD_{rms} is one order of magnitude smaller than that of without flow control (Figure 13a). In addition, a large portion of the OPD_{rms} values are smaller than 0.01 μm, indicating that the laser beam can maintain its quality as it propagates through the wake region behind the turret.

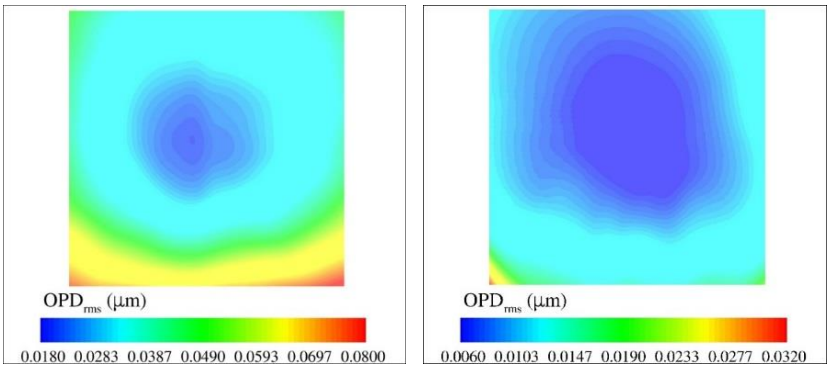

a) without bleed b) with bleed

Figure 13 Root-mean-squared of OPD at 135° viewing angle

Although the conceptual bleed design (Figure 8) was demonstrated to be effective in reducing the degradation of the laser beam in numerical simulations, the performance of this bleed slot configuration was based on a trial-and-error approach.[6] As discussed earlier, a design methodology was developed to optimize the bleed flow path to reduce the drag of the system, and various configurations can be developed based on prescribed width, depth, and length, as shown Figure 14. Although the elliptical bleed design provided an aerodynamic profile (Figure 14a), the intersection of the cylindrical turret base to the elliptical shape created an upward convex contour on the side of the cavity. This profile tends to push the flow upward causing it to interact with the wake region behind the turret, which generates more disturbance. A flat base was modeled to eliminate this undesired flow feature, as depicted in Figure 14b. However, the numerical results did not demonstrate significant improvement. In addition, it is difficult to transition from a square shape to an elliptical contour. Therefore a simpler ramp configuration (Figure 14c) was tested to determine its capability in reducing the wake region behind the hemispherical turret.

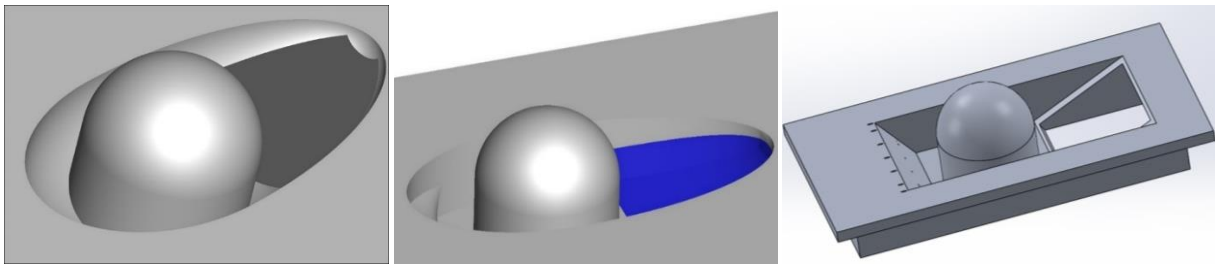

a) elliptical design b) canoe design c) ramp design

Figure 14 Different conceptual bleed configurations using the design methodology

The numerical simulations show that the ramp configuration decreases the wake region behind the hemispherical turret with the bleed system, as illustrated in Figure 15. A reduction of the flow separation indicates the quality of the laser beam on the target has improved dramatically. Note that the numerical shadowgraph images were extracted 0.4″ from the bottom wall, which will allow for comparison with the water-table flow visualization. However, this apparatus is still under construction in the AFRL/Directed Energy Directorate at Kirtland AFB, NM.

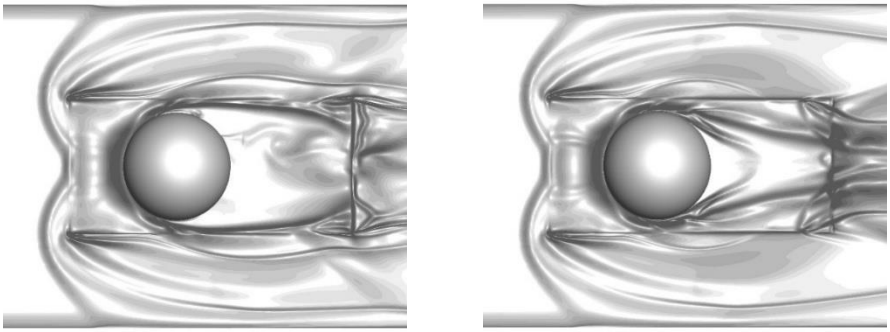

a) without bleed b) bleed

Figure 15 Top view of the numerical shadowgraph images for bleed-ramp design

SUMMARY

Numerical simulations were performed to study the effects of bleed flow control for aero-optics in a Mach 2 flow. The first conceptual bleed design showed that this technique could reduce the OPD_{rms} for the 45º looking forward and 135º viewing downstream of the hemispherical turret. The numerical results indicate that this flow control system could significantly improve the quality of the laser beam on the target.

A bleed design methodology was developed to reduce the overall drag of the flow path based on the inviscid assumption. Three different bleed configurations, including an ellipse, canoe and ramp, were numerically simulated to determine their effectiveness in decreasing the wake region behind the turret and thereby improving the quality of the laser beam on the target. The numerical solutions demonstrate that the ramp configuration performs best out of the three bleed configurations studied. These numerical findings will be validated through a water table surface flow visualization, using an experimental water table apparatus currently under construction at the AFRL/Directed Energy Directorate in Kirtland AFB, NM.

References

1. Sutton, G.W., "On Optical Imaging Through Aircraft Turbulent Boundary Layers," AIAA Paper 1980-1413, 1980.
2. Sutton, G.W., "Aero-optical Foundations and Applications," AIAA Journal, Vol. 23, No. 10, pp 1525-1537.
3. Siegenthaler, J.P, Jumper, E. J., and Gordeyev, S., "Atmospheric Propagation Vs. Aero-Optics," AIAA Paper 2008-1076, 2008.
4. Clark, R., Banish, M., and Hammer, J., "Fundamentals of Aero-Optics Phenomena," AIAA Paper 1994-2545, 1994.
5. Tam, C.-J., Madden, T.J., Wittich, D.J., Noren, C.A., Carnrike, D., Kumar, R., and Gogineni, S., “Investigations of Supersonic Flow over a Hemispherical Turret using Numerical Simulations,” AIAA Paper 2016-3225, 2016.
6. Tam, C.-J. and Madden, T.J., “Numerical Investigations of Transonic Flow over a Hemisphere using Various Turbulence Models,” 18th Annual Directed Energy Symposium, Albuquerque, 2016.
7. Connors, T.R., “Predicted Performance of a Thrust-Enhanced SR-71 Aircraft with an External Payload,” NASA Technical Memorandum 104330, Edwards, California, 1997.
8. Tam, C.-J., Hsu, K.-Y., Gruber, M.R., and Behdadnia, R., “Investigations of Shock/Boundary Layer Control in Scramjet Isolator,” JANNAF 54th Joint Propulsion Meeting, 2007.

9. Tam, C.-J., Hsu, K.-Y., Gruber, M.R., and Behdadnia, R., "Numerical and Experimental Studies of Shock Control using Boundary Layer Bleed in Axisymmetric Scramjet Isolator," JANNAF 30th Airbreathing Propulsion Subcommittee, 2008.
10. Eberhard, R. W., "The Design and Construction of a Free Surface Water Table for the Investigation of Compressible-Flow Phenomenon," Thesis Paper for MS, Virginia Polytechnic Institute, 1956.
11. Preiswerk, E., "Application of the Methods of Gas Dynamics to Water Flows with Free Surface," NACA Technical Memorandum 935, 1940.
12. Orlin, W. J., Linder, N.J., and Bitterly, J.C., "Application of the Analogy Between Water Flow with a Free Surface and Two-Dimensional Compressible Gas Flow," NACA Report 875, 1947.
13. Shapiro, A., "Free Surface Water Table," Physical Measurements in Gas Dynamics and Combustion, 1st ed., H. Taylor, Ed. Princeton: Princeton University Press, pp. 314. 1954.
14. Sultanova, N., Kasarova, S., and Nikolov, I., "Dispersion Properties of Optical Polymers", *Acta Phys. Pol. A*, vol. 116, no. 4, pp. 585-587, 2009.
15. Luke, E.A. and Cinnella, P., "Numerical Simulations of Mixtures of Fluids using Upwind Algorithms," *Computers & Fluids*, 2007, 36(10), pp 1547-1566.
16. Luke, E.A. and George, T., "Loci: a Rule-Based Framework for Parallel Multidisciplinary Simulation Synthesis," *Journal of Functional Programming*, 2005, 15(3), pp 477-502.